

**TECHNICAL REPORT STANDARD PAGE**

1. Report No. <b>FHWA/ LA. 03 / 376</b>		2. Government Accession No.	3. Recipient's Catalog No.
4. Title and Subtitle <b>Nondestructive Evaluation of Fiber Reinforced Polymer Bridges and Decks</b>		5. Report Date <b>October 2003</b>	
		6. Performing Organization Code	
7. Author(s) <b>Dr. Paul Ziehl and William S. Bane</b>		8. Performing Organization Report No.	
9. Performing Organization Name and Address <b>Dept. of Civil and Environmental Engineering Tulane University New Orleans, Louisiana 70118</b>		10. Work Unit No.	
		11. Contract or Grant No. <b>State Project Number: 736-99-1137 LTRC Project Number: 03-1TUL</b>	
12. Sponsoring Agency Name and Address <b>Louisiana Transportation Research Center 4101 Gourrier Avenue Baton Rouge, LA 70809</b>		13. Type of Report and Period Covered <b>Final Report Period Covered: July 2002- June 2003</b>	
		14. Sponsoring Agency Code	
15. Supplementary Notes			
<p><b>16. Abstract</b></p> <p>The research described herein involved both nondestructive evaluation and destructive testing of an FRP honeycomb specimen. The specimen is representative of an FRP bridge that is to be constructed in Troupsburg, New York. The specimen was tested in fatigue at Clarkson University prior to its arrival at Tulane University. The specimen was loaded and unloaded at Tulane University on several different occasions spanning a period of four months. Strain, load, displacement, and acoustic emission were monitored. A finite element model of the specimen was developed and this model was compared to the measured displacement data.</p>			
17. Key Words <b>Fiber Reinforced Polymers, FRP, Honeycomb, bridges, fatigue, strain, load, displacement, acoustic emissions, strain gauges, data acquisition.</b>		18. Distribution Statement <b>Unrestricted. This document is available through the National Technical Information Service, Springfield, VA 21161.</b>	
19. Security Classif. (of this report) <b>N/A</b>	20. Security Classif. (of this page) <b>N/A</b>	21. No. of Pages <b>62</b>	22. Price



# **Nondestructive Evaluation of Fiber Reinforced Polymer Bridges and Decks**

by

William S. Bane  
Paul H. Ziehl, Ph.D., P.E.

Dept. of Civil and Environmental Engineering  
Tulane University  
New Orleans, Louisiana 70118

LTRC Project No. 03-1TUL  
State Project No. 736-99-1137

conducted for

Louisiana Department of Transportation and Development  
Louisiana Transportation Research Center

The contents of this report reflect the views of the author/principal investigator who is responsible for the facts and the accuracy of the data presented herein. The contents do not necessarily reflect the views or policies of the Louisiana Department of Transportation and Development or the Louisiana Transportation Research Center. This report does not constitute a standard, specification, or regulation.

October 2003



## **ABSTRACT**

The research described herein involved both nondestructive evaluation and destructive testing of an FRP honeycomb specimen. The specimen is representative of an FRP bridge that is to be constructed in Troupsburg, New York. The specimen was tested in fatigue at Clarkson University prior to its arrival at Tulane University. The specimen was loaded and unloaded at Tulane University on several different occasions spanning a period of four months. Strain, load, displacement, and acoustic emission were monitored. A finite element model of the specimen was developed and this model was compared to the measured displacement data.



## **ACKNOWLEDGMENTS**

The research described in this report was supported by the Louisiana Department of Transportation and Development (LA DOTD) Support Program for Senior Projects in Civil Engineering. The funds from this program were instrumental in obtaining portions of the data acquisition and other equipment that were vital for the successful completion of the project. We would like to thank Michael Boudreaux of the Louisiana Transportation Research Center (LTRC) for the support, direction, and encouragement that he offered during the project. We would also like to thank Walid Alaywan and Harold “Skip” Paul of the LTRC and Paul Fossier of the LA DOTD for their interest, input, and support.



## **IMPLEMENTATION STATEMENT**

Fiber reinforced polymers (FRP) are quickly finding their way into the transportation infrastructure. These materials are inherently different from concrete and steel. Therefore, it is not surprising that some early pioneering applications have experienced difficulty. These difficulties can be lessened to a large degree through the development of an appropriate nondestructive evaluation method for FRP materials applied to the infrastructure.

The LA DOTD and LTRC will benefit from this research in that experience with FRP components for the civil infrastructure will be gained. Of equal importance, a nondestructive test procedure will be developed that will be useful for not only the monitoring of FRP components but also for the evaluation of more conventional construction materials such as reinforced and prestressed concrete. A group of senior students was involved in the experimental testing and the analysis of the acoustic emission data. This effort was lead by William Bane, who gave an oral presentation regarding the research to a group of faculty, graduate and undergraduate students. The students gained experience through exposure to new construction techniques, materials, and nondestructive evaluation procedures. The senior students involved plan to pursue careers in civil engineering and benefited greatly from their interaction with personnel from the LA DOTD and LTRC.



# TABLE OF CONTENTS

ABSTRACT.....	iii
ACKNOWLEDGMENTS .....	v
IMPLEMENTATION STATEMENT .....	vii
LIST OF TABLES .....	xiii
INTRODUCTION.....	1
OBJECTIVES .....	3
SCOPE .....	5
METHODOLOGY.....	7
Description of the Test Specimen .....	7
Test Setup and Instrumentation.....	9
Loading Procedure .....	17
December 10, 2002 - Loading to 16,200 pounds .....	17
December 18, 2002 Test #1 - Loading to 23,000 pounds .....	17
December 18, 2002 Test #2 - Loading to 26,000 pounds .....	17
February 6, 2003 - Loading to 25,000 pounds .....	17
February 10, 2003 - Loading to 56,000 pounds .....	17
February 13, 2003 - Loading to 84,000 pounds .....	18
March 14, 2003 - Loading to Failure (82,000 pounds).....	18
Finite Element Modeling .....	19
DISCUSSION OF RESULTS.....	21
Load, Strain, and Displacement .....	21
February 10, 2003 - Loading to 56,000 pounds .....	21
March 14, 2003 - Loading to Failure (82,000 pounds).....	21
Acoustic Emission .....	22
December 10, 2002 - Loading to 16,200 pounds .....	26
December 18, 2002 Test #1 - Loading to 23,000 pounds .....	26
December 18, 2002 Test #2 - Loading to 26,000 pounds .....	27
February 6, 2003 - Loading to 25,000 pounds .....	27
February 10, 2003 - Loading to 56,000 pounds .....	28
February 13, 2003 Test #1 - Loading to 70,000 pounds .....	28
February 13, 2003 Test #2 - Loading to 84,000 pounds .....	29
CONCLUSIONS.....	41
ACRONYMS, ABBREVIATIONS, & SYMBOLS .....	45
REFERENCES .....	47



## LIST OF FIGURES

Figure 1 Honeycomb bridge system and sinusoidal core.....	11
Figure 2 Plan view of proposed bridge - load case 1 .....	11
Figure 3 Test specimen dimensions.....	12
Figure 4 Face sheet laminate schedule.....	12
Figure 5 Delaminations of specimen prior to testing.....	13
Figure 6 Strain Gauge locations.....	13
Figure 7 Schematic of test set up - elevation .....	14
Figure 8 Schematic of test set up - end view .....	14
Figure 9 Photograph of test set up - prior to loading .....	15
Figure 10 Photograph of test set up - during loading.....	15
Figure 11 Photograph of test set up - during loading.....	16
Figure 12 Acoustic emission sensor locations .....	16
Figure 13 Loading profile - February 10, 2003.....	22
Figure 14 Loading profile - February 10, 2003.....	22
Figure 15 Measured displacement - February 10, 2003.....	23
Figure 16 Loading profile - March 14, 2003.....	23
Figure 17 Measured strains - March 14, 2003 .....	24
Figure 18 Measured displacements - March 14, 2003 .....	24
Figure 19 Amplitude vs. time - December 10, 2002.....	30
Figure 20 Amplitude vs. time - December 18, 2002 (loading No. 1) .....	30
Figure 21 Amplitude vs. time - December 18, 2002 (loading No. 2) .....	31
Figure 22 Amplitude vs. time - February 6, 2003.....	31
Figure 23 Amplitude vs. time - February 10, 2003.....	32
Figure 24 Amplitude, channel, time - February 10, 2003 (during holds) .....	32
Figure 25 Amplitude, channel, time - February 10, 2003 (entire test).....	33
Figure 26 Amplitude vs. time - February 13, 2003 (loading No. 1) .....	33
Figure 27 Amplitude, channel, time - loading of February 13, 2003 (loading No. 1, during holds).....	34
Figure 28 Amplitude, channel, time - loading of February 13, 2003 (loading No. 1, entire test) .....	34
Figure 29 Vertical displacement at 6,000 pounds - pin and roller supports .....	38
Figure 30 Vertical displacement at 82,000 pounds - pin and roller supports .....	38
Figure 31 Vertical displacement at 6,000 pounds - bearing pad supports .....	39
Figure 32 Vertical displacement at 82,000 pounds - bearing pad supports .....	39



## LIST OF TABLES

Table 1 Face sheet lamina description .....	8
Table 2 Face sheet lamina material properties .....	8
Table 3 Core lamina material properties .....	9
Table 4 Equivalent face sheet material properties .....	20
Table 5 Equivalent core material properties .....	20
Table 6 Midspan deflection .....	37



## INTRODUCTION

During the last several decades it has become apparent that bridges constructed with conventional materials have inherent drawbacks for certain applications. Fiber reinforced polymers (FRP) are being used increasingly for new construction and the rehabilitation of existing structures. Some advantages offered by FRPs include high strength-to-weight ratio, resistance to corrosion, and the ability to be mass produced in virtually any shape. Several fabrication processes are currently in use including resin infusion, contact molding, and pultrusion. Each of these processes has inherent limitations and advantage

As FRPs find their way into the civil infrastructure, it will be imperative to establish a means of assessing the quality of the original product and monitoring the product during its service life. In the pressure vessel and piping industries, these materials have been used in structural applications for over 40 years. During the 1970s, a series of vessel failures occurred with sometimes catastrophic results. These failures necessitated the development and implementation of a nondestructive evaluation method. The most suitable method was found to be acoustic emission monitoring. Evaluation procedures and codes were subsequently developed that incorporated this method [1-3].

Acoustic emission monitoring is a sensitive global test technique that can be used to detect significant damage as it occurs in a structure. Due to the advent of high-speed affordable computing and advances in digital signal processing and pattern recognition techniques, acoustic emission monitoring continues to develop at a rapid pace. It is therefore likely that acoustic emission monitoring will be an integral part of the design process and the structural health monitoring of FRP components for use in civil applications. Acoustic emission monitoring is also being used to establish life cycle predictions of reinforced concrete bridges and evaluate of bridges that have been strengthened with FRPs [4-6].



## **OBJECTIVES**

Objectives of the research were as follows:

1. Conduct experimental testing of a large-scale FRP honeycomb specimen that is representative of an actual bridge to be constructed in New York.
2. Monitor the behavior of the specimen during loading. Parameters to be monitored included acoustic emission, strain, load, and displacement.
3. Develop a finite element model of the test specimen.
4. Interpret the acoustic emission data and draw conclusions about the suitability of this test method for the nondestructive evaluation of FRP components for civil infrastructure applications.



## **SCOPE**

The scope of this report includes the experimental testing of the large-scale FRP honeycomb specimen and the presentation of relevant data gathered as a result of the testing. A finite element model was developed and the development of this model is also included in the scope of this report.

This project is not a conventional research project but rather a senior research project. Therefore, this report is somewhat limited. Aspects of this project that are not addressed here are more fully documented in a Master's thesis [7] and a report to the New York Department of Transportation [8]. Further documentation will be available in the form of two journal articles that are currently in preparation [9, 10].



## METHODOLOGY

The FRP beam specimen was evaluated through the monitoring of acoustic emission, load, displacement, and strain. The specimen was loaded on several different occasions. On the final occasion, the hydraulic rams were extended to their full stroke of 6 inches and held until failure of the specimen occurred. The methodology is addressed in four parts: description of the test specimen, test setup and instrumentation, loading procedure, and finite element modeling.

### Description of the Test Specimen

In the case of FRP structural systems for the transportation infrastructure, it is often the case that system stiffness and low cost are competing parameters. The least expensive structural systems are typically E-glass based FRP materials. Since the stiffness of E-glass reinforced laminates is generally in the range of 1.0 to 3.0 msi, the stiffness of the system must be achieved through its geometry.

In 1996, Kansas Structural Composites, Inc. fabricated and installed the first FRP bridge in the United States [11]. This bridge took advantage of the structural efficiency of the honeycomb system. With this system, the top and bottom face sheets act as the primary flexural elements. These elements are separated by a structurally efficient honeycomb core. The honeycomb core is not a true honeycomb, but is rather a system of “flats” and sinusoidal “flutes” (Figure 1). The primary fiber reinforcement in the facesheets is oriented longitudinally to achieve the greatest stiffness.

For calculation purposes, simplification of this honeycomb core geometry is made using micro-mechanics to transform the sinusoidal core material into a solid representative volume element. This process is described in more detail later.

Kansas Structural Composites, Inc. of Russell, Kansas provided the test specimen. The specimen had previously been tested by Dr. Maria Lopez of Clarkson University in fatigue loading up to 2 million cycles. The cyclic load ranged from 2.0 to 12.0 kips total load. The geometry of the specimen was based on the geometry of a proposed bridge to be constructed in New York. The overall depth of the beam specimen was 35 inches and 0.50 inch thick faceskins were used. The test specimen is representative of an approximately 1 foot wide strip of the proposed bridge under HS-25 wheel loading (shown schematically in Figure 2). Finite element modeling performed at Tulane University indicated that faceskins on the exterior spans of the proposed bridge of 1.0 inches thickness and 0.75 inch thickness for interior spans were desirable for certain load cases. Further information on the finite element

modeling of the proposed bridge can be found in references [7] and [8]. The width of the Tulane test specimen was 13.5 inches and the length was 32 feet 0 inches (figure 3).

Material properties of the Tulane beam specimen were found through experimental testing of representative coupon specimens at Clarkson University [12]. Material properties obtained by testing of coupon specimens are not necessarily representative of the actual properties of the test specimen. Nonetheless, the testing of coupon specimens is a common procedure in the FRP industry. Descriptions of the face sheet constituent layers are given in table 1 and material properties of the face sheets and core material are given in table 2 and table 3. The face sheet layout diagram is shown in figure 4.

When the specimen arrived at Tulane, it had several delaminations between the honeycomb core and the exterior flats that formed the sides of the specimen. It is unclear whether these delaminations were due to the fatigue testing that took place at Clarkson University or if it occurred during shipping. The test specimen delaminations upon arrival at Tulane University are shown schematically in figure 5.

**Table 1**  
**Face sheet lamina description**

Ply Name	Ply Type	Nominal Weight, w (oz./ft <sup>2</sup> )	Thickness, t (in)	Volume Fraction, V <sub>f</sub>
Bonding Layer	ChopSM	3.0	0.082	0.1726
CM3205	0°	16/9	0.0245	0.3428
CM3205	90°	16/9	0.0245	0.3428
CM3205	ContSM	0.5	0.01	0.2359
UM1810	0°	2.0	0.025	0.3774
UM1810	ContSM	1.0	0.0132	0.3582

**Table 2**  
**Face sheet lamina material properties**

Ply Name	Orientation	E <sub>1</sub> (x 10 <sup>6</sup> psi)	E <sub>2</sub> (x 10 <sup>6</sup> psi)	G <sub>12</sub> (x 10 <sup>6</sup> psi)	G <sub>23</sub> (x 10 <sup>6</sup> psi)	ν <sub>12</sub>	ν <sub>23</sub>
Bond Layer	Random	1.41	1.41	0.507	0.308	0.394	0.401
CM3205	0° or 90°	4.02	1.16	0.447	0.417	0.295	0.390
CM3205	Random	1.71	1.71	0.610	0.343	0.402	0.400
UM1810	0°	4.36	1.24	0.479	0.447	0.293	0.386
UM1810	Random	2.31	2.31	0.820	0.430	0.409	0.388
Core Mat	Random	1.71	1.71	0.611	0.431	0.402	0.388

**Table 3**  
**Core lamina material properties**

Laminate Orientation	$E_1/E_2$ (x $10^6$ psi)	$\nu_{12}$	$G_{12}$ (x $10^6$ psi)	Shear Strength (x $10^6$ psi)	sult. (tension) (x $10^6$ psi)	eult. (tension) ( $\mu\epsilon$ )	sult. (compr.) (x $10^6$ psi)	eult. (compr.) ( $\mu\epsilon$ )	a (coeff. of thermal exp.)
Core	1.102	0.30	0.450	0.0102	0.0165	15,000	0.00392	3,550	$28.1 \times 10^{-6}$

### Test Setup and Instrumentation

The beam specimen was initially placed on its side to allow for the application of strain gages to the bottom face, at mid-span, and underneath each loading point. Two types of strain gages were used; both were manufactured by Vishay Measurements Group. The two types were CEA-06-250UW-120 and CEA-06-500UW-120. Both types were 120 Ohm resistance. The 500UW gages were larger than the 250UW gages and were used for the majority of the beam with the 250UW gages being used as redundant gages.

The strain gages were applied using a two-part AE-10 epoxy also manufactured by Measurements Group. A layer of epoxy was applied to the surface of the beam and allowed to cure. The cured epoxy was then sanded and cleaned with rubbing alcohol, and then the gage was applied to the epoxy surface with the same two-part epoxy. After the gage had cured to the beam, the three lead wires were soldered to the gage. The strain gages were then weatherproofed a Teflon tape coating and a butyl rubber patch and covered with a neoprene pad. The location of the strain gages is shown in figure 6.

After the majority of the strain gages were affixed to the beam specimen, it was rotated and placed on 26" by 26" by 32" reinforced concrete pedestals with 0.79" by 12.5" by 22" elastomeric bearing pad supports. Once the beam was placed upright on the pedestals the loading frames were placed over the loading points and bracing frames were attached to the loading frame to prevent the beam from buckling laterally more than 1/4" during testing. A bearing pad identical to the ones placed under the end supports was placed at each loading point and covered by a steel plate of one-inch thickness and identical plan dimensions.

Four string pots (a spring-coiled wire used to measure linear displacements) were placed underneath the beam: one under each loading point, one at midspan, and one at the southern bearing pad. The purpose of the string pot at the location of the support was to measure the

deflection of the bearing pad under loading; the other three string pots measured the deflection of the beam including the deflection of the bearing pad. Load was applied to the specimen by means of two hydraulic rams having 100-kip capacity and 6-inch stroke. Load was measured with calibrated 100-kip capacity load cells. Schematics of the beam test setup including the dimensions of the loading points are shown in figures 7 and 8. Photographs of the test setup and beam specimen are shown in figures 9 through 11.

Load, displacement, and strain measurements were recorded with a 24-channel IOTech conditioned signal system. Measurements were recorded continuously throughout all tests at a frequency of one reading per second.

Eight acoustic emission (AE) sensors were affixed to the center of the top facesheet at the locations shown in figure 12. Hot melt glue was used as the couplant. All AE sensors were type R15I manufactured by Physical Acoustics Corporation (PAC). These sensors are resonant and contain a 40 dB integral pre-amplifier. Acoustic emission was monitored continuously throughout each test. All acoustic emission signals were monitored with an 8-channel DiSP system also manufactured by PAC. This is a portable system that is digital and has source location, pattern recognition, and waveform storage capability.

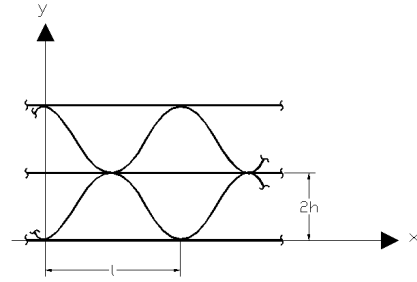


**Figure 1**  
**Honeycomb bridge system and sinusoidal core**

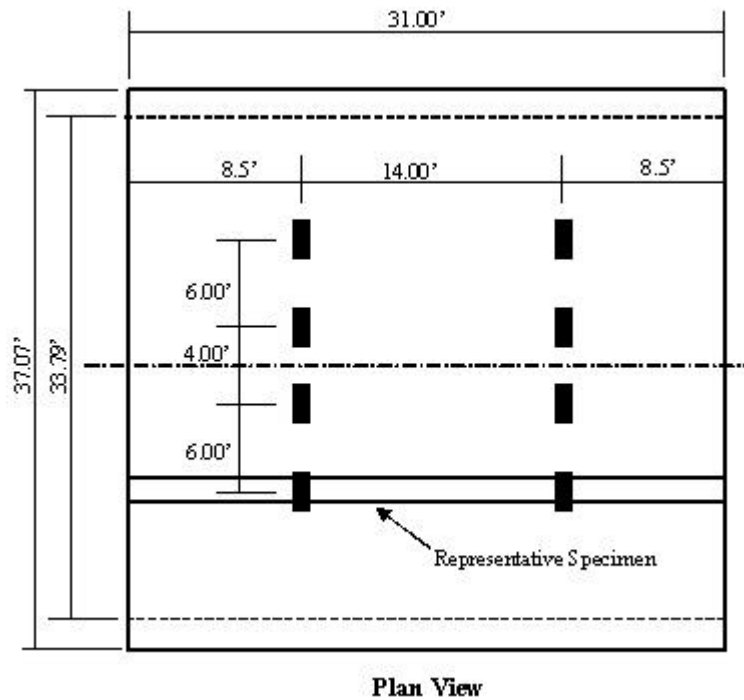


**Figure 2**  
**Plan view of proposed bridge - load case 1**

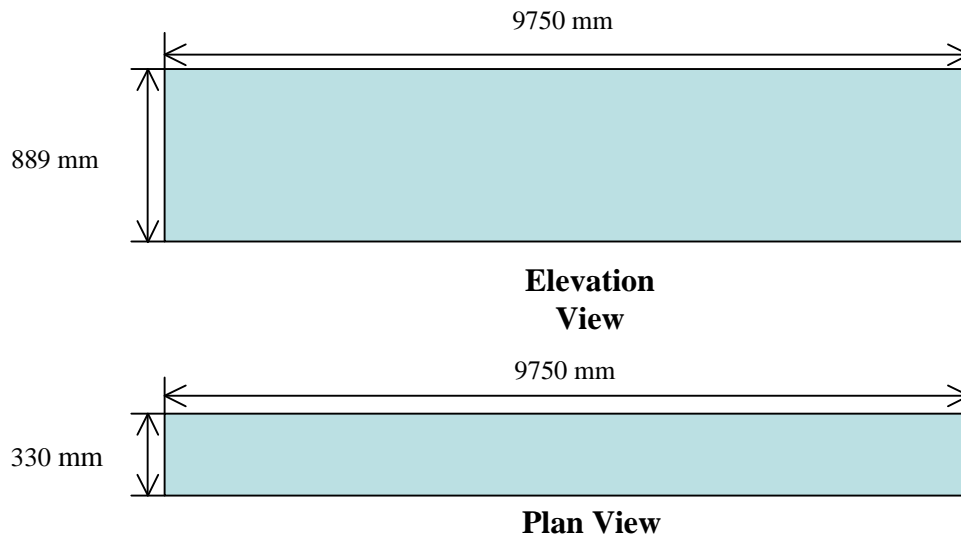


**Figure 3**  
**Test specimen dimensions**

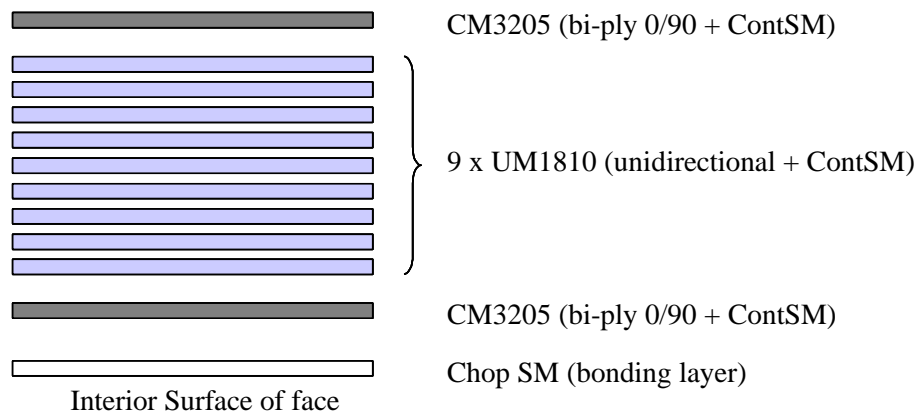


**Figure 4**  
**Face sheet laminate schedule**

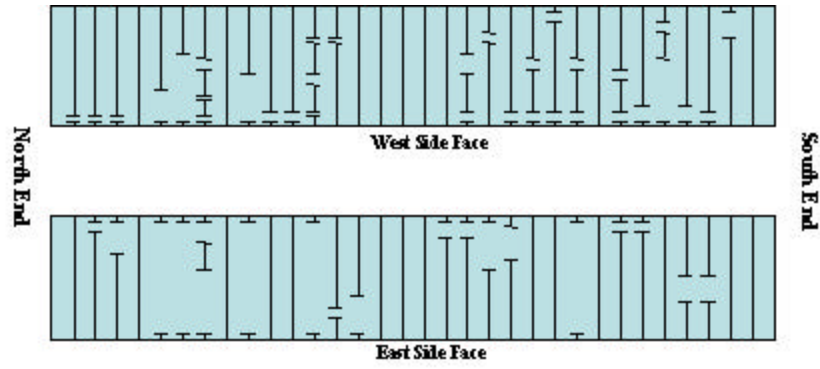


**Figure 5**  
Delaminations of specimen prior to testing

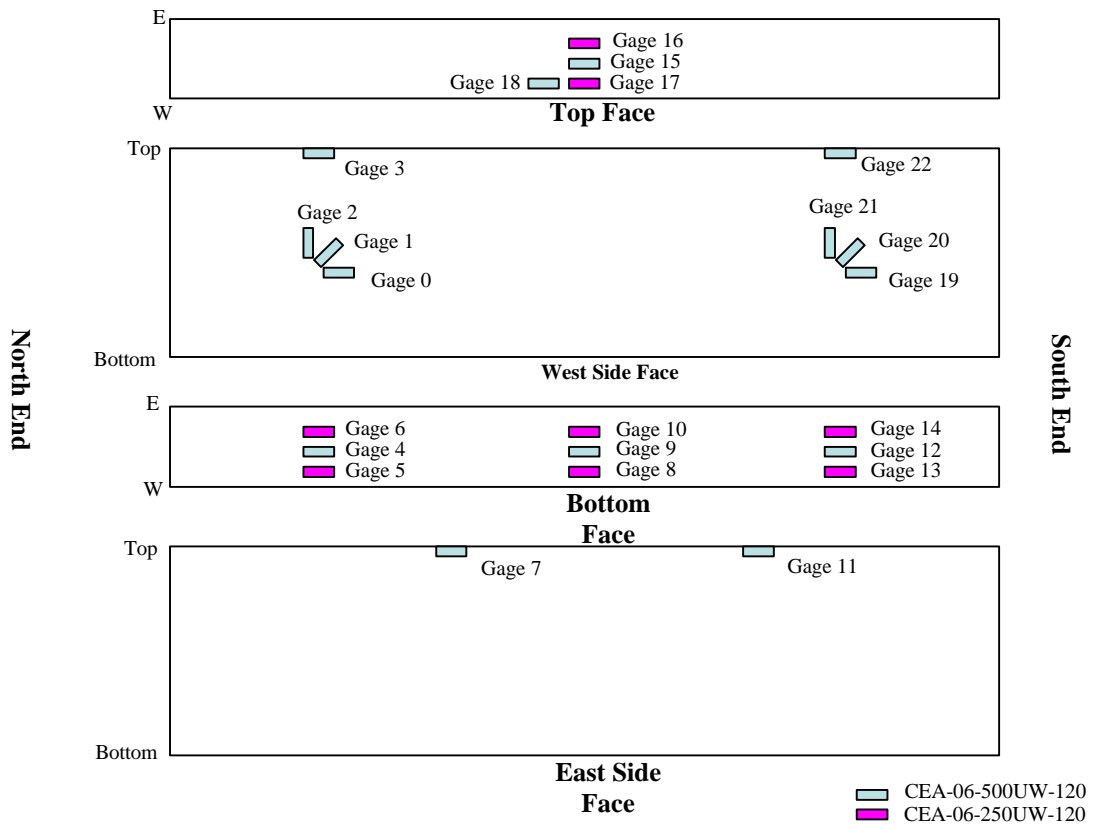


**Figure 6**  
Strain Gauge locations

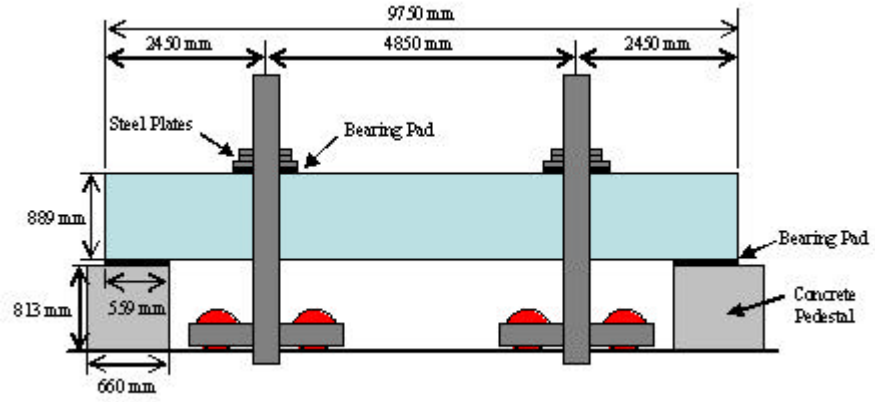


**Figure 7**  
**Schematic of test set up - elevation**

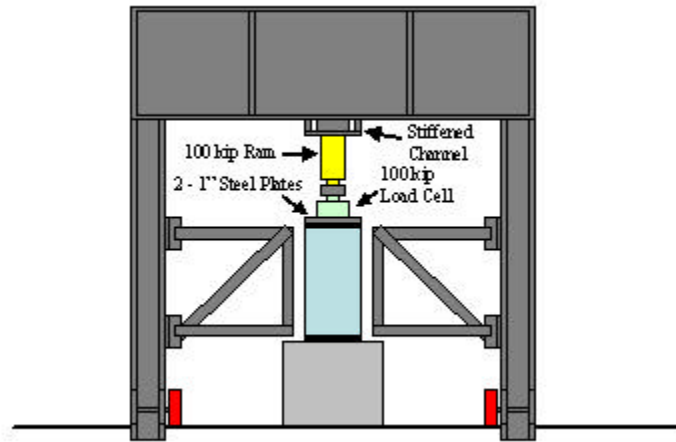


**Figure 8**  
**Schematic of test set up - end view**



**Figure 9**  
**Photograph of test set up - prior to loading**



**Figure 10**  
**Photograph of test set up - during loading**



**Figure 11**  
**Photograph of test set up - during loading**

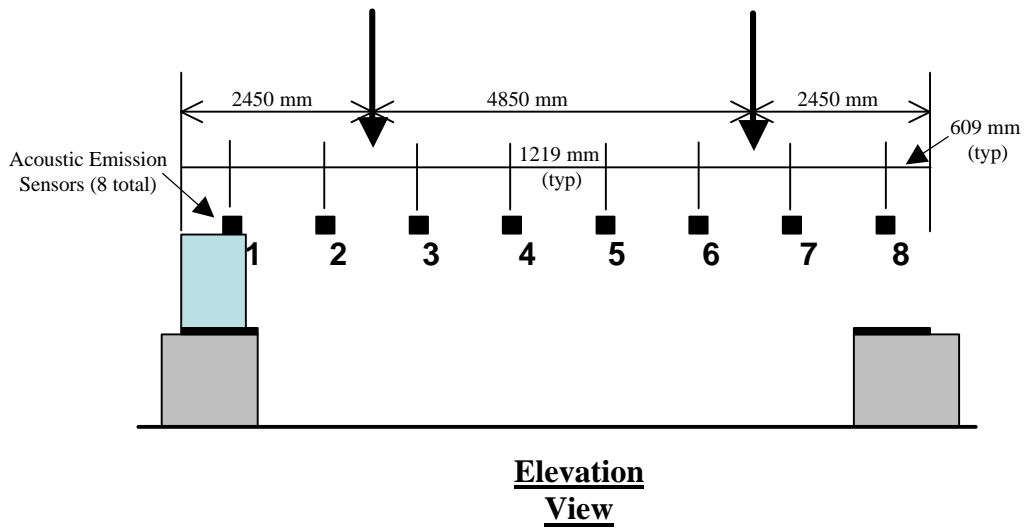


**Figure 12**  
**Acoustic emission sensor locations**

## **Loading Procedure**

The specimen was originally loaded on December 10, 2002. It was then reloaded to higher levels of load on several different occasions. The loading and reloading procedure was necessary to aid in the generation of meaningful acoustic emission data and the interpretation of that data. The loadings are briefly described. In all cases, the load refers to the load at each loading point as opposed to the total load on the specimen.

### **December 10, 2002 - Loading to 16,200 pounds**

As with subsequent loadings, the loading on this date was performed in a stair-step manner to aid in the generation of meaningful acoustic emission data. The reasons for this are described in the results section of this report. The electrically gathered strain, load, and displacement data from this test was lost due to an unexpected loss of power during the test. However, the acoustic emission data was saved and a test log was generated during the test that included the manually gathered midspan deflection and load data.

### **December 18, 2002 Test #1 - Loading to 23,000 pounds**

After adding a backup power source (uninterrupted power supply) to the system, two more tests were performed on this date. The first of these tests took the specimen up to 23,000 pounds using a series of stepped loadings with 3,000-pound increments up to 20,000 pounds and then an unloading cycle back to 15,000 pounds. The specimen was then taken to 23,000 pounds.

### **December 18, 2002 Test #2 - Loading to 26,000 pounds**

The specimen was completely unloaded and then reloaded the same day using 10,000 pound and then 2,000- pound increments up to 26,000 pounds.

### **February 6, 2003 - Loading to 25,000 pounds**

The specimen was loaded incrementally to 25,000 pounds on this date and then fully unloaded. Due to a problem with corruption of the data, electrically recorded load, strain, and displacement information is not available. The acoustic emission data was saved and is discussed later. Manually recorded displacement and load information is available.

### **February 10, 2003 - Loading to 56,000 pounds**

The first attempt at loading the beam to failure was conducted on this date. The beam was loaded to 10,000 pounds using 5,000-pound increments before a series of experimental difficulties necessitated unloading of the specimen. After addressing the difficulties, the specimen was loaded to 35,000 pounds using 5,000-pound increments and then unloaded back to 30,000 pounds. The loading was then continued up to 50,000 pounds with another 5,000 pound unloading at 45,000 pounds.

During the load hold at 50,000 pounds, the midspan string pot disconnected from the beam and had to be reattached necessitating an unloading to 40,000 pounds before reloading to 50,000 pounds. During the next 5,000- pound load increment to 55,000 pounds, the north frame's loading apparatus began to slip and the strengthened channel that the hydraulic ram was bolted to collapsed.

A new loading setup was devised using solid plates to eliminate the weak point of the setup. Many solid steel plates were also added on top of the original loading plate to minimize eccentricities in the loading apparatus.

### **February 13, 2003 - Loading to 84,000 pounds**

After putting the new loading apparatus in place, a second attempt to load the beam to failure was conducted on this date. This loading involved many loading and unloading cycles before reaching a maximum load of 70,000 pounds.

The specimen was completely unloaded after reaching 70,000 pounds and the loading apparatus was checked to make sure it was lined up properly. The specimen was then reloaded. The beam was loaded to 50,000 pounds first and then an attempt to fail the beam was made. The rams reached their maximum stroke of 6 inches at 84,000 pounds, where the beam was held for 15 minutes before unloading and reloading to the maximum stroke two more times.

### **March 14, 2003 - Loading to Failure (82,000 pounds)**

The specimen was brought back to the maximum sustainable load, which at this point was 82,000 pounds, and held until the specimen failed. This decision was made for two reasons. First, the specimen was very close to its ultimate load as indicated by previous test results on similar specimens and the presence of visible and audible damage to the specimen. Second, the progression of the damage and the amount of time the specimen could withstand this very high level of load was of interest.

The test to failure was performed on March 14, 2003. The load was stepped up to 82,000 pounds. The maximum of 84,000 pounds previously obtained was not obtained in this loading. This can be attributed to damage accumulation in the specimen leading to lower stiffness and/or changes in experimental conditions.

## Finite Element Modeling

FRP is not an isotropic material so creating a simplified formulaic approach for predicting behavior is not straightforward. One method of predicting behavior is the use of micro-mechanics and lamination theory to develop a system of equations for specimen behavior such as deflection, stress, and strain. Another is to use the finite element method to perform these calculations.

When finite element models are developed, one consideration is the number of elements to be used in the model. While it is possible to model structures to a very high degree of detail, this will significantly increase the time required to run the model. Therefore, simplification is desirable if it does not adversely affect the results. In the case of honeycomb structures, it is desirable to replace the complex geometry of the flats and flutes with a solid representation of this geometry. This approach is referred to as the Representative Volume Element (RVE) approach since a representative portion of the structure is used to determine material properties of the entire structure or portion of the structure. The RVE approach has been successfully applied to honeycomb core geometry in the past and this approach is detailed in reference [13].

The finite element modeling was accomplished using Abaqus [14], a finite element analysis program from Hibbitt, Karlsson & Sorenson. Patran [15], a mesh generation program, was used to construct the models before they were analyzed in Abaqus. Two types of models were constructed. The first type involved accurate geometric representations of a honeycomb beam structure and used measured material properties that were obtained from coupon testing. The second type of model used solid sections to replace the complex geometry of the honeycomb core. Material properties were developed based on measured material properties and the (RVE) method. Both approaches are described in detail in reference [7]. Only the RVE model is discussed here.

The properties of the facesheets were developed by lamination theory and are given in table 4. The representative material properties used for the honeycomb core were calculated using the method developed by Davalos, et. al. [13]. These properties are given in table 5.

**Table 4**  
**Equivalent face sheet material properties**

Laminate Orientation	$E_1$ (x $10^6$ psi)	$\nu_{12}$	$G$ (x $10^6$ psi)	Shear Strength (x $10^6$ psi)	$s_{ult}$ (tension) x $10^6$ psi	$e_{ult}$ (tension ) ( $\mu\epsilon$ )	$e_{ult}$ (compr.) ( $\mu\epsilon$ )	$s_{ult}$ (compr.) x $10^6$ psi	$a$ (coeff. of thermal exp.)
0°	3.191	0.2 6	0.696	0.0141	0.0615	19,300	0.0348	10,900	$16.2 \times 10^{-4}$
90°	1.436	0.1 8	0.696	0.0141	0.0127	8,900	-	-	$36.2 \times 10^{-4}$

**Table 5**  
**Equivalent core material properties**

	$E_x$ (x $10^6$ psi)	$E_y$ (x $10^6$ psi)	$E_z$ (x $10^6$ psi)	$G_{xy}$	$G_{xz}$	$G_{yz}$	$\nu_{xy}$	$\nu_{xz}$	$\nu_{yz}$
Equivalent Core Properties	$0.0449 E_1$	$8.36 \times 10^{-5} E_1$	$0.107 E_2$	$5.98 \times 10^{-5} E_1$	$0.0765 G_{12}$	$0.030 G_{12}$	0.431	0.169	$0.273 \times 10^{-4}$
Numerical Value	0.049480	$9.2 \times 10^{-5}$	0.117914	$6.6 \times 10^{-5}$	0.034425	0.0135	0.431	0.169	$0.273 \times 10^{-4}$

## **DISCUSSION OF RESULTS**

The discussion of results is addressed in three parts: 1) load, strain, and displacement, 2) acoustic emission, and 3) finite element modeling.

### **Load, Strain, and Displacement**

For the sake of brevity, only the loadings of February 10, 2003 (55,000 pounds) and the final loading of March 14, 2003 (82,000 pounds) are discussed. Since the behavior of the FRP specimen was close to linear, the other loadings had similar results. All loadings and the data gathered from the other loadings are described in reference [7].

#### **February 10, 2003 - Loading to 56,000 pounds**

The loading profile for this loading is shown in Figure 13. The midspan strains at 56,000 pounds were approximately 5,000 micro-strains; both tensile and compressive as shown in figure 14.

The deflection of the beam specimen under 56,000 pounds at each loading point was 4.50" as shown in figure 15. This deflection includes the deflection of the bearing pad.

#### **March 14, 2003 - Loading to Failure (82,000 pounds)**

This loading profile is shown in figure 16. The maximum of 84,000 pounds previously obtained was not obtained in this loading. This can be attributed to damage accumulation in the specimen leading to lower stiffness and/or changes in experimental conditions. The strains reached in this loading are shown in figure 17. The maximum strain at midspan was 9,200 micro-strain in compression and 7,600 micro-strain in tension.

The maximum recorded deflection at midspan was 7.2 inches, which includes the bearing pad deflection, as shown in figure 18.

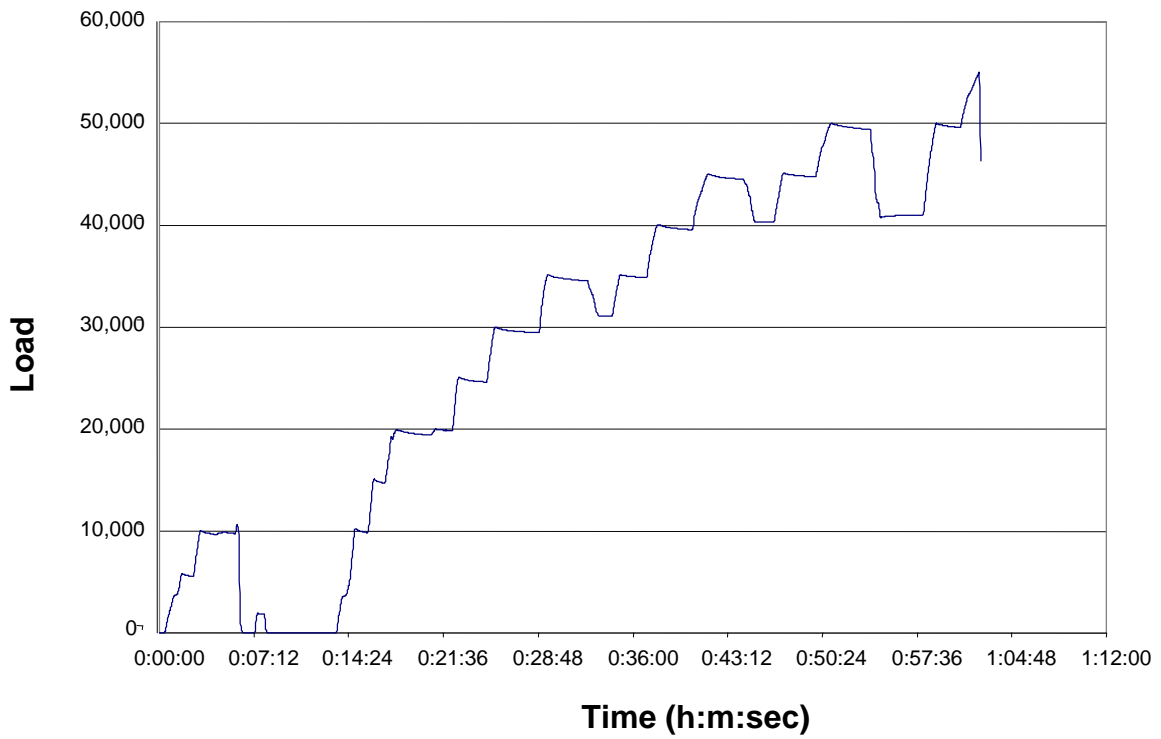


**Figure 13**  
**Loading profile - February 10, 2003**

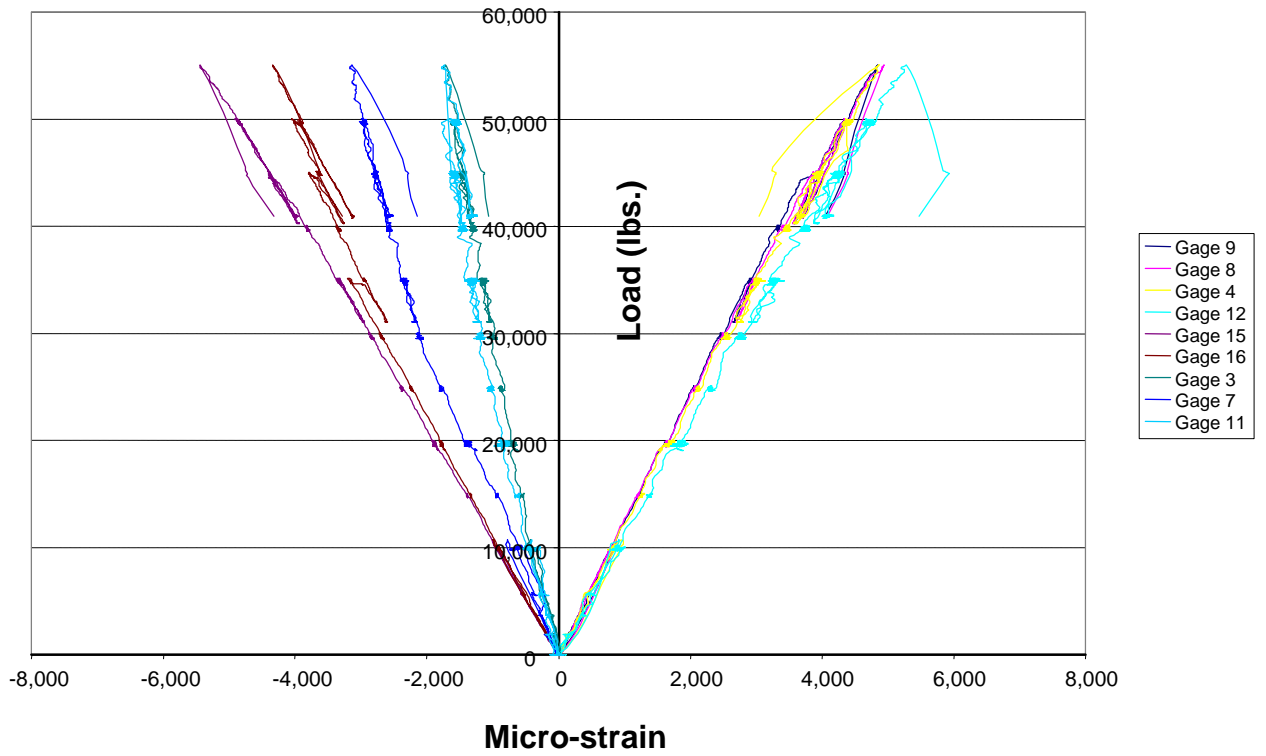


**Figure 14**  
**Loading profile - February 10, 2003**

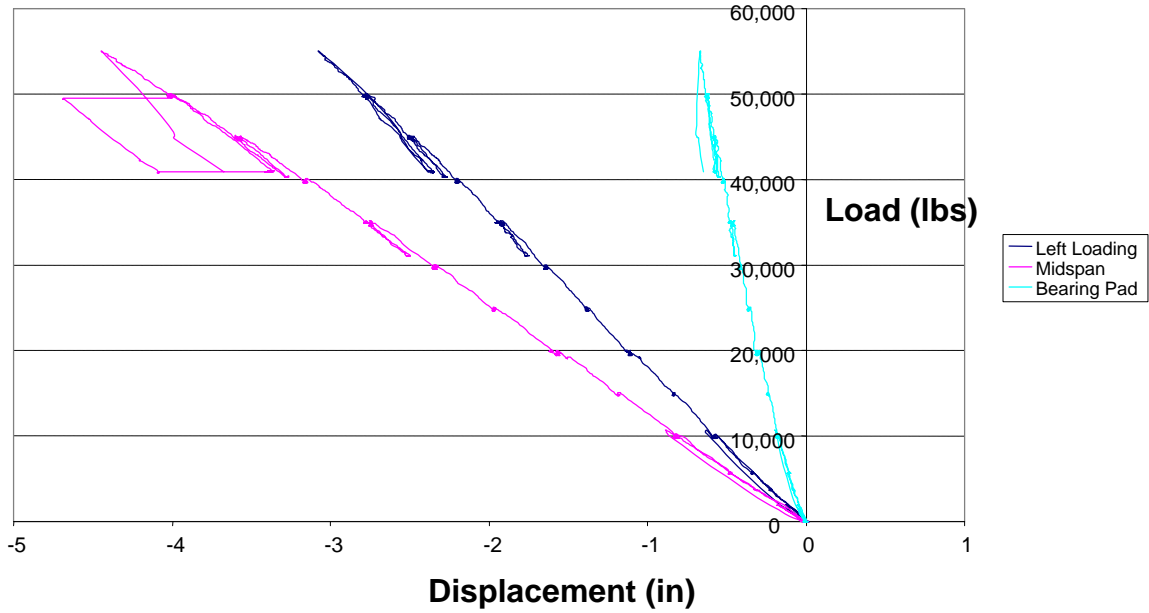


**Figure 15**  
**Measured displacement - February 10, 2003**

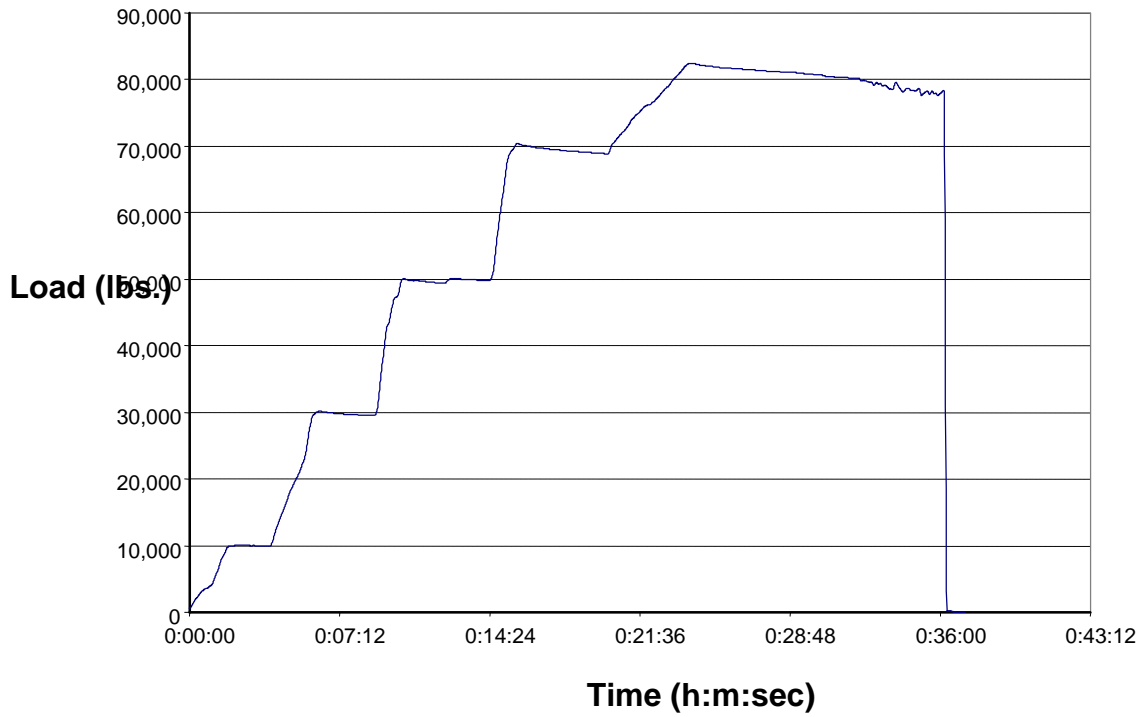


**Figure 16**  
**Loading profile - March 14, 2003**

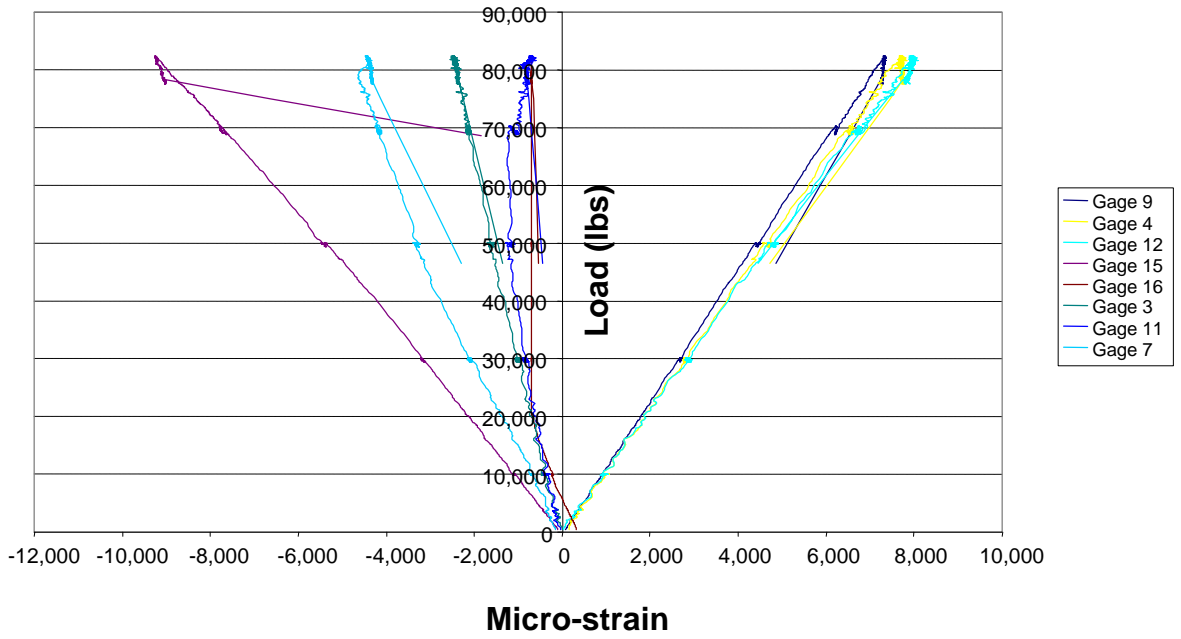


**Figure 17**  
**Measured strains - March 14, 2003**

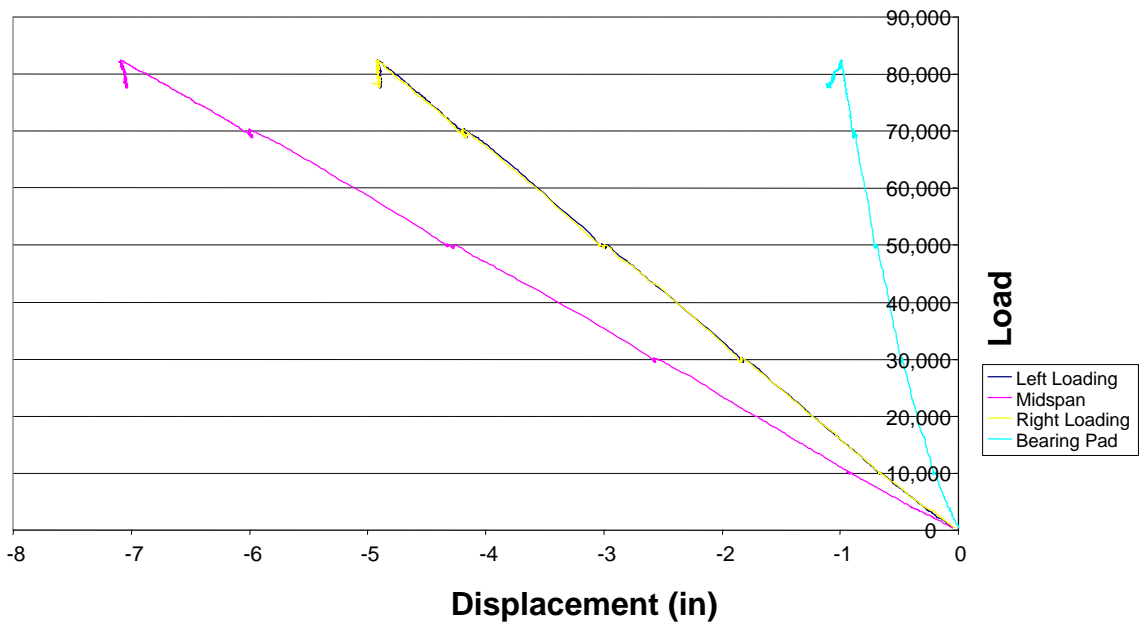


**Figure 18**  
**Measured displacements - March 14, 2003**

## Acoustic Emission

As described previously, eight acoustic emission sensors were applied to the top facesheet. More sensors would have been advantageous for better coverage of the specimen. However, at the time of testing, the instrumentation was limited to eight channels. Twenty-four channels would have been preferred and this number has been used on similarly sized FRP specimens in the past [16, 17]. Since previous testing conducted elsewhere had generally culminated in detachment of the top face sheet from the honeycomb core material [12], all eight sensors were placed along the top of the specimen. These sensors were evenly spaced along the length of the specimen and centered on the longitudinal axis (figure 12).

For interpretation of acoustic emission data, a large number of parameters can be selected. Some of these include amplitude, duration, event rate, counts, signal strength, and historic index. Definitions of acoustic emission terms can be found in ASTM E-137 [18]. When the goal of the acoustic emission analysis is to determine levels of damage or correlations with fitness for service, methods that are based on the pattern of acoustic emission activity combined with information about the loading history of the specimen have been used effectively in many industries including those related to FRP piping, tanks, pressure vessels, and manlift booms. This technique has also been used extensively in the aerospace and marine industries.

Other methods of interpreting data are often based on digital signal processing techniques. Because these methods tend to be based on the frequency content of the recorded information, broadband sensors are necessary for correct application of these techniques. The use of broadband sensors on large specimens is not always practical due to the lower sensitivity of these sensors when compared to their resonant counterparts. Other drawbacks of broadband sensors include high cost and low durability.

One parameter that has been found to be particularly effective in determining the onset of damage in FRP specimens is the Felicity ratio [18, 19]. This ratio can be defined as (load at onset of significant acoustic emission activity) / (previous level of load). Emissions during load holds have also been correlated to damage in FRP specimens and in many cases, emissions during holds tend to occur as the Felicity ratio first drops below unity. These two parameters, Felicity ratio and emissions during holds, are the focus of the acoustic emission analysis described in this report.

Emissions can be located using a number of methods. One-, two-, and three- dimensional source location techniques are available. One-dimensional methods are often based on the

time of arrival of the recorded signal. Two-dimensional methods are often based on time of arrival combined with triangulation. The most reliable method of source location for large scale specimens is by activity of individual channels and this method was utilized for the analysis described in this report.

To aid in the interpretation of acoustic emission data, a series of loading and reloading increments is necessary. Each loading and the acoustic emission activity that was generated due to this loading is discussed below.

### **December 10, 2002 - Loading to 16,200 pounds**

The first loading of the specimen took place on December 10, 2002. The loading schedule is superimposed on a plot of acoustic emission amplitude versus time in figure 19. The amplitude versus time plot is generated for all eight channels on a single graph. It is possible to view the acoustic emission activity on a per channel basis, but the general trends of the acoustic emission activity were of primary interest. As mentioned previously, acoustic emission activity in FRPs is load history dependent. Therefore, the previous level of load to which the specimen was subjected is shown on all acoustic emission plots with a red dashed line. For this initial loading, the largest level of load to which the specimen was subjected was the fatigue loading of 6,000 pounds at each point load.

As seen in the figure, the load was increased monotonically up to a level of approximately 5,600 pounds and was then held for a period of approximately three minutes. The hold at 5,600 pounds was inserted in the loading procedure to establish the presence or lack of a Felicity effect due to the fatigue loading. Five acoustic emission hits were recorded during the hold. The largest amplitude hit recorded was 68 dB. Although the single acoustic emission hit of 68 dB is noteworthy, this level of activity in a large-scale specimen is generally not considered to be substantial

The specimen was then loaded beyond this level in a stair step manner to a maximum load of 16,200 pounds. There was very little acoustic emission activity during the holds preceding that at 15,800 pounds. During the load hold at 15,800 pounds, a significant amount of activity was recorded. This activity was repeated during the load hold at 16,200 pounds. Due to the continuing activity during these load holds, the load was removed from the specimen, and it was allowed to recover for eight days under a state of no load.

### **December 18, 2002 Test #1 - Loading to 23,000 pounds**

The specimen was loaded on two separate occasions on December 18, 2002. A plot of acoustic emission amplitude versus time for the first loading on this date is shown in Figure

20. As before, the level of load to which the specimen had been previously subjected is shown with a dashed red line at 16,200 pounds.

Very little acoustic emission activity was present during the load hold at 2,800 pounds. Some activity was present during the load holds at 6,000 and 8,000 pounds; however, all hits during these holds were below 60 dB. Subsequent load holds below 16,200 pounds had very little in the way of acoustic emission activity. Relatively high amplitude hits of 70 dB were recorded during the hold at 18,000 pounds, which is in excess of the previous level of loading. Continuing emission was recorded during the load hold at 20,000 pounds. Due to the continuing emission during the hold, the load was decreased and then increased to 19,000 pounds. At this level, similar acoustic emission activity to that seen during the hold at 6,000 pounds was recorded. Notable and continuing acoustic emission activity was recorded during the holds at 22,000 and 23,000 pounds. Due to the ongoing emission during these holds, the specimen was unloaded and allowed to recover for a few hours prior to reloading on this same date.

#### **December 18, 2002 Test #2 - Loading to 26,000 pounds**

The specimen was reloaded on this same date. A plot of acoustic emission amplitude versus time for the reloading is shown in figure 21. Ideally, prior to reloading a specimen, a conditioning period of at least 12 hours under no load is used. Previous research has shown that if this conditioning period is not used, the reloading will be less acoustically active than if the conditioning period were present [20]. The codes which govern the acoustic emission testing of fiber reinforced vessels require such a conditioning period between loadings.

Very little in the way of acoustic emission activity was recorded during the holds at loads below 23,000 pounds. Once the level of load was increased above 23,000 pounds continuing emission during the holds was again recorded. Therefore, the specimen was unloaded and allowed to recover for a period well in excess of 12 hours. The next loading occurred in February of 2003.

#### **February 6, 2003 - Loading to 25,000 pounds**

A plot of acoustic emission amplitude versus time for the reloading on this date is shown in Figure 22. This loading was conducted primarily as a trial run to verify the status of the testing apparatus and the data acquisition system.

Prior to the load hold at 20,000 pounds very little acoustic emission activity was recorded during the load holds. At the load hold at 20,000 pounds, a notable amount of activity took place with one hit of 72 dB. At the load hold of 25,000 pounds, notable activity was again recorded with one hit of 67 dB.

### **February 10, 2003 - Loading to 56,000 pounds**

The first attempt to load the specimen to failure took place on this date. A plot of acoustic emission amplitude versus time for this loading is shown in Figure 23.

An extended load hold at 10,000 pounds was used at the beginning of this loading for purposes of adjustment of the testing apparatus. The adjustment process caused a good deal of acoustic emission activity and this non-genuine emission is labeled in the plot. The load hold at 20,000 pounds resulted in very little activity. The activity again increased as the previous level of load (26,000 pounds) was exceeded. The amount of activity recorded during the load hold at 35,000 pounds was very significant and continued throughout the hold. For this reason, the load was reduced and then increased again to 35,500 pounds. During this load hold at 35,500 pounds, the emission again continued and was significant. Although it could be argued that the Felicity effect was present to some degree at lower levels of load, this was the first strong indication of a Felicity effect and therefore this portion of the plot is marked with an arrow. The load was increased in a stair step manner to a level of 45,000 pounds and then reduced and increased to 45,000 pounds again. As expected, the Felicity effect was again clearly present at this level of load. It was also present at 50,000 pounds.

Three-dimensional plots of amplitude, channel, and time are shown for the load holds during the return loadings to 35,000 and 45,000 pounds in figure 24. These figures give an indication of where the majority of the damage was generated during these load holds. Channels 4 and 6 were the most active during the hold at 35,000 pounds. These same channels were again the most active during the hold at 45,000 pounds. As shown in figure 12, these channels were located inside the loading points. A similar plot was generated for the entire duration of the test as shown in figure 25. This figure indicates that channel 4 was the most active followed by channel 7.

### **February 13, 2003 Test #1 - Loading to 70,000 pounds**

The second attempt to fail the specimen took place on this date. A plot of acoustic emission amplitude versus time for this reloading is shown in Figure 26.

Stepped loading and unloading was again used in an attempt to determine damage as shown in figure 26. The activity again increased significantly when the previous level of load (56,000 pounds) was exceeded. The Felicity effect was clearly present as determined by continuing significant emission during the load hold at 40,000 pounds. This portion of the plot is shaded. The Felicity effect was again clearly present at the next load hold of 50,000 pounds.

Three-dimensional plots of amplitude, channel, and time are shown for the load holds during the initial loadings to 40,000 and 50,000 pounds in figure 27. These figures indicate where the majority of the damage was generated during these load holds. Channels 2 and 5 were the most active during the hold at 40,000 pounds. Channel 7 was the most active during the load hold 50,000 pounds. As shown in figure 12, these channels were located just outside the loading points. A similar plot was generated for the entire duration of the test as shown in figure 28. This figure indicates that channel 2 was the most active followed by channels 5, 6, and 7.

**February 13, 2003 Test #2 - Loading to 84,000 pounds**

Based on the level of acoustic emission activity during the previous series of loading steps, an explosive failure of the test specimen was expected in excess of 70,000 pounds. All sensors were therefore removed from the test specimen prior to this loading.

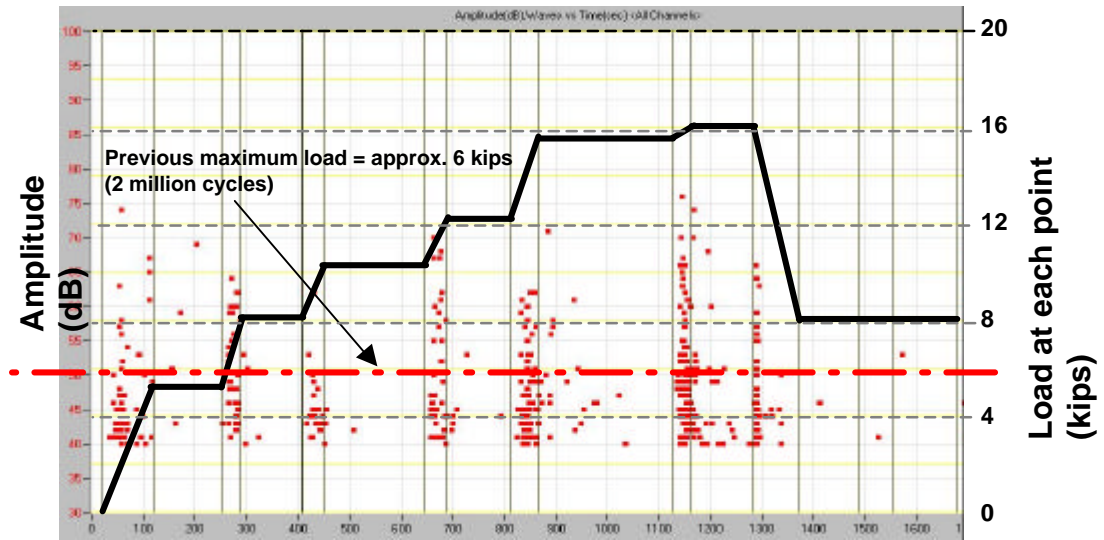


**Figure 19**  
**Amplitude vs. time - December 10, 2002**

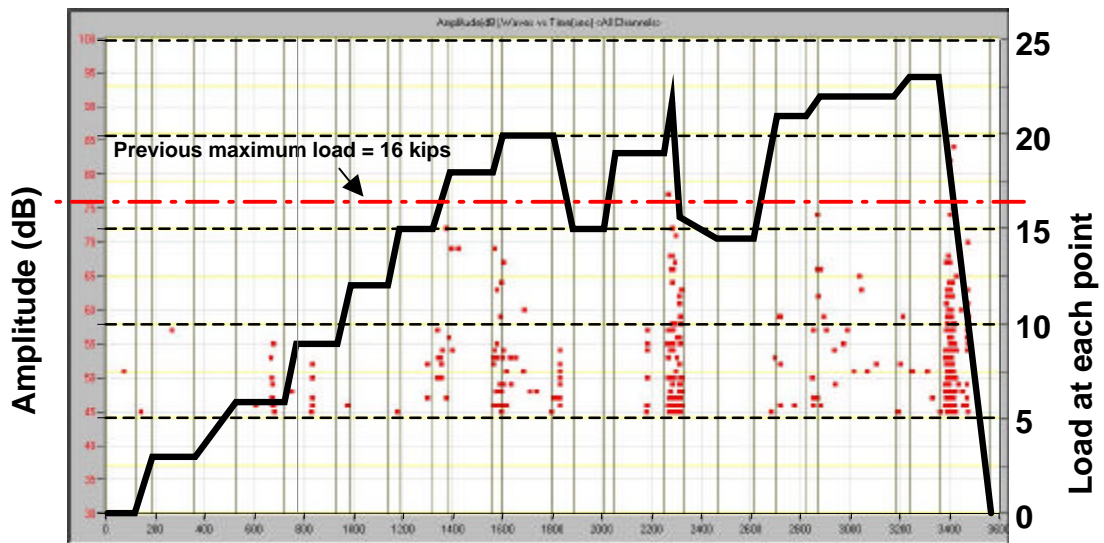


**Figure 20**  
**Amplitude vs. time - December 18, 2002 (loading No. 1)**

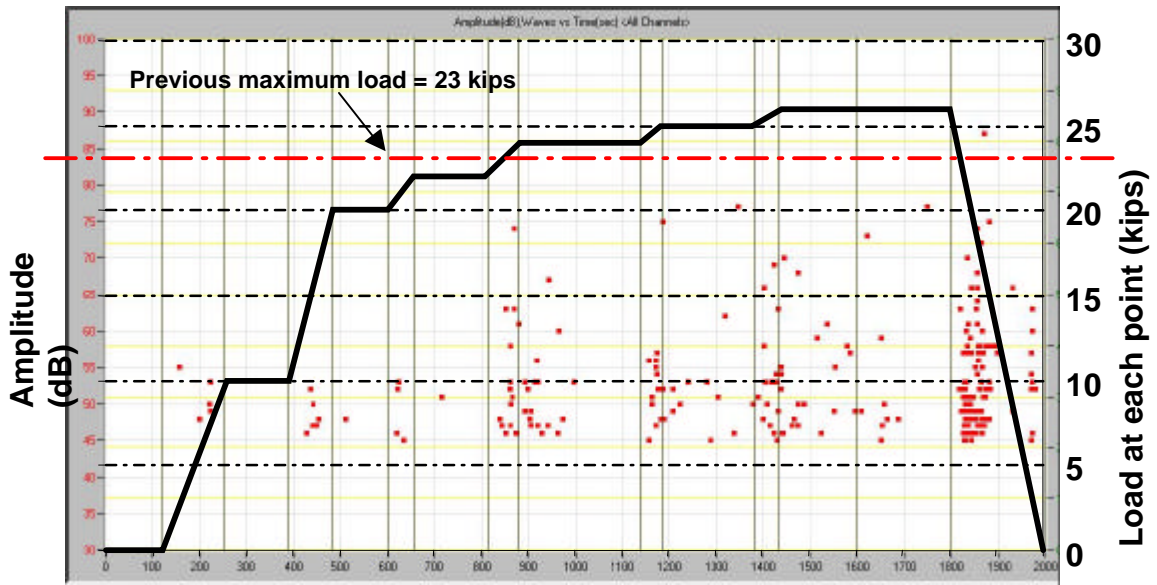


**Figure 21**  
**Amplitude vs. time - December 18, 2002 (loading No. 2)**

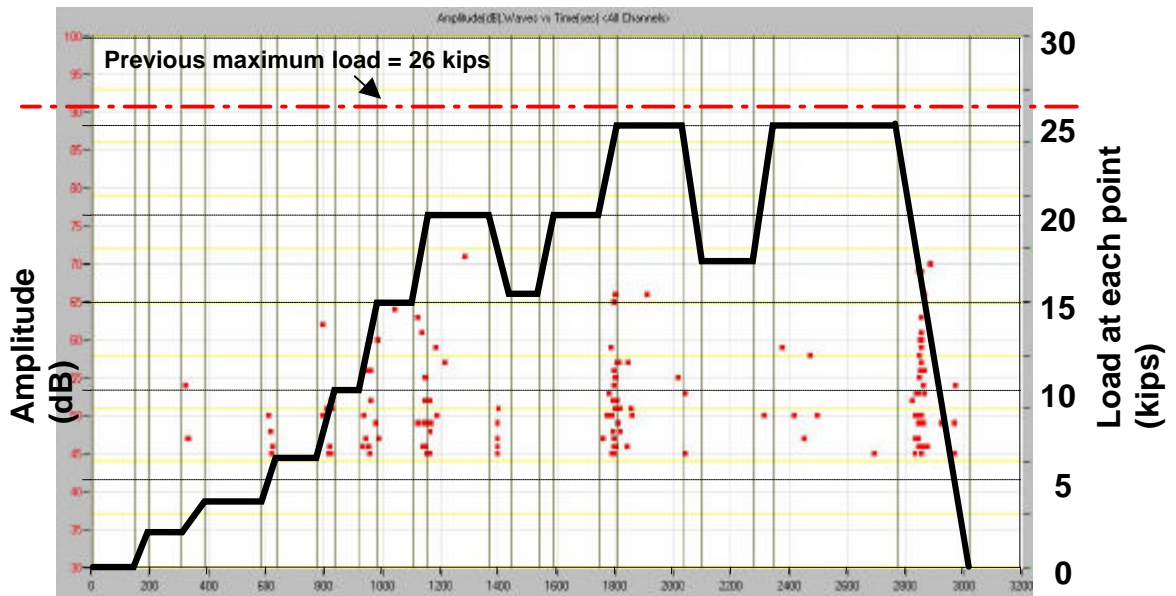


**Figure 22**  
**Amplitude vs. time - February 6, 2003**

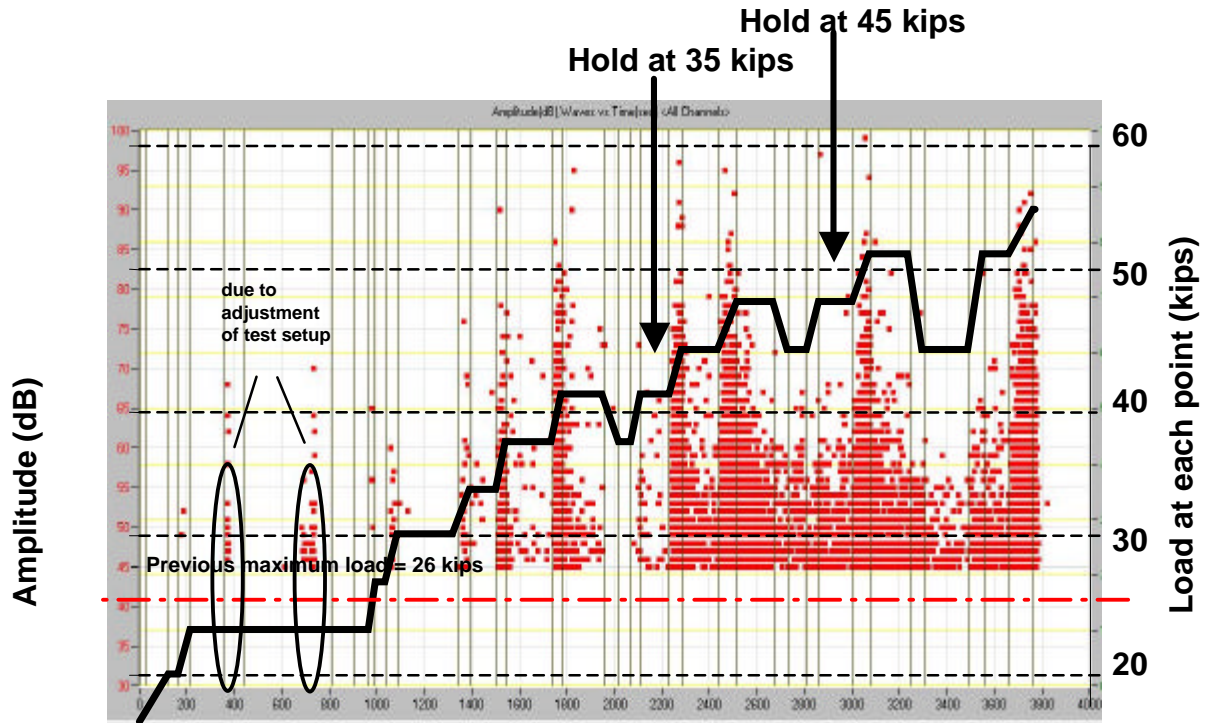


Figure 23

Amplitude vs. time - February 10, 2003

Hold at 35  
kips

Hold at 45  
kips

0

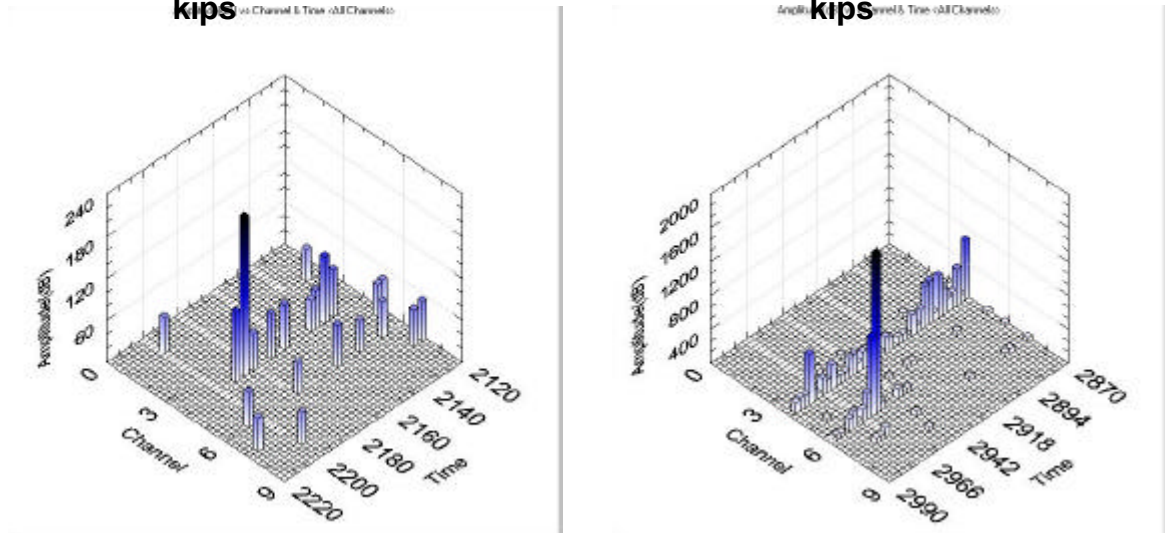
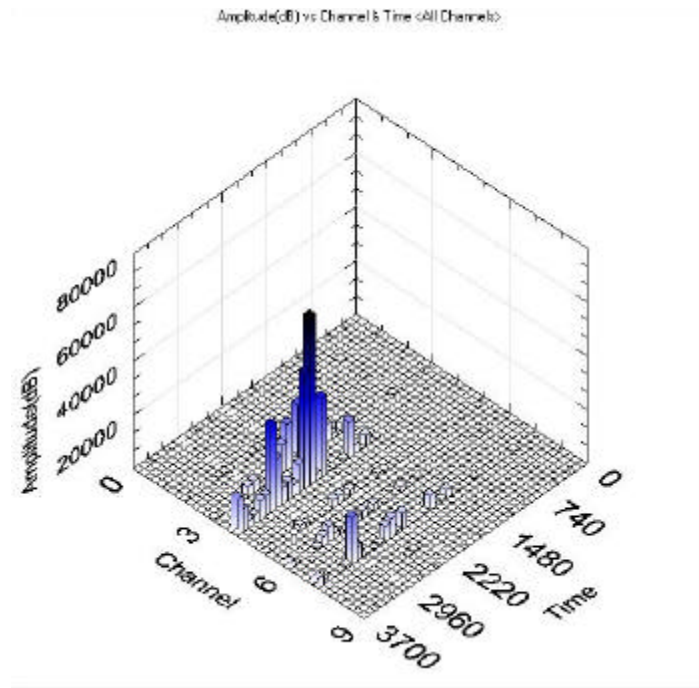
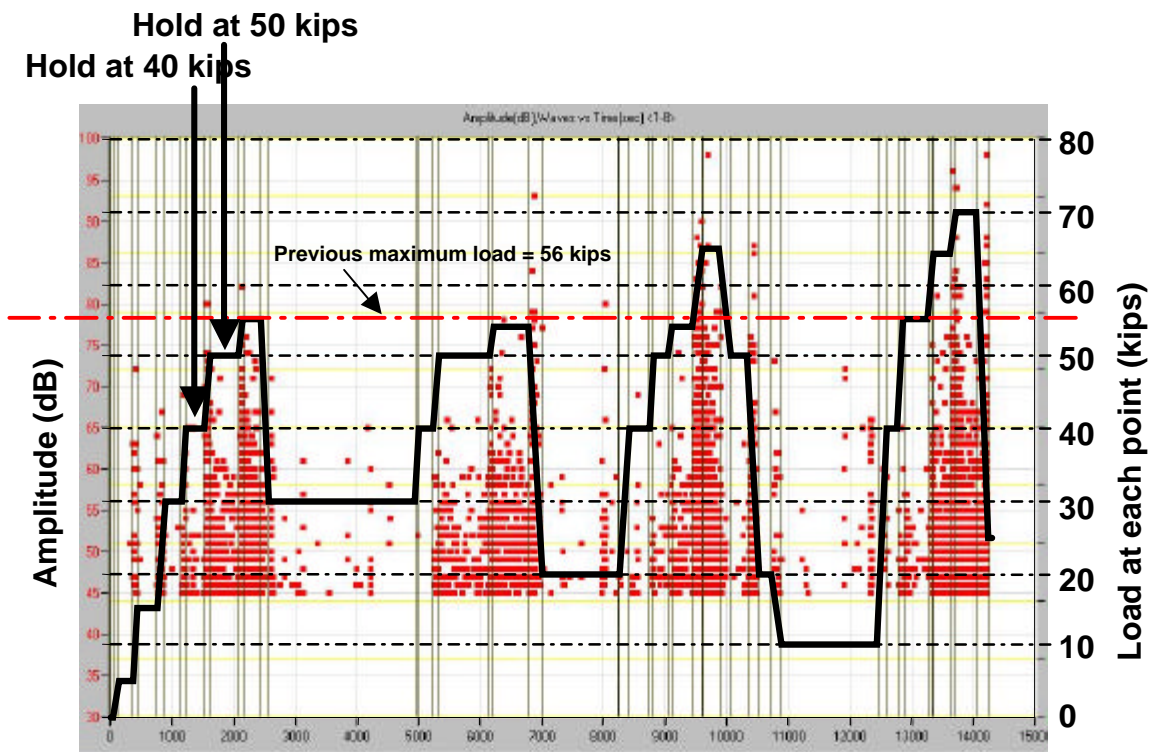


Figure 24

Amplitude, channel, time - February 10, 2003 (during holds)

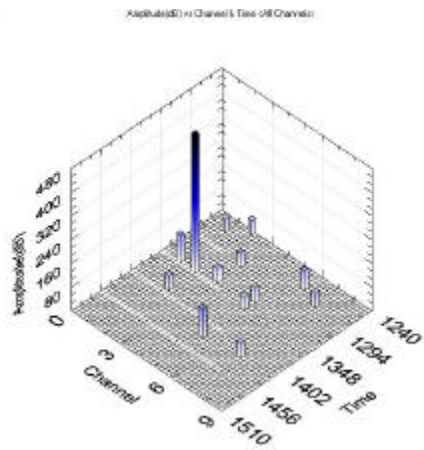


**Figure 25**  
Amplitude, channel, time - February 10, 2003 (entire test)



**Figure 26**  
Amplitude vs. time - February 13, 2003 (loading No. 1)

### Hold at 40 kips



### Hold at 50

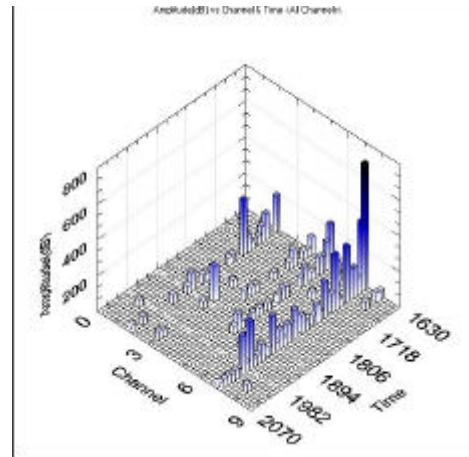


**Figure 27**  
Amplitude, channel, time - loading of February 13, 2003 (loading No. 1, during holds)

### Entire Test

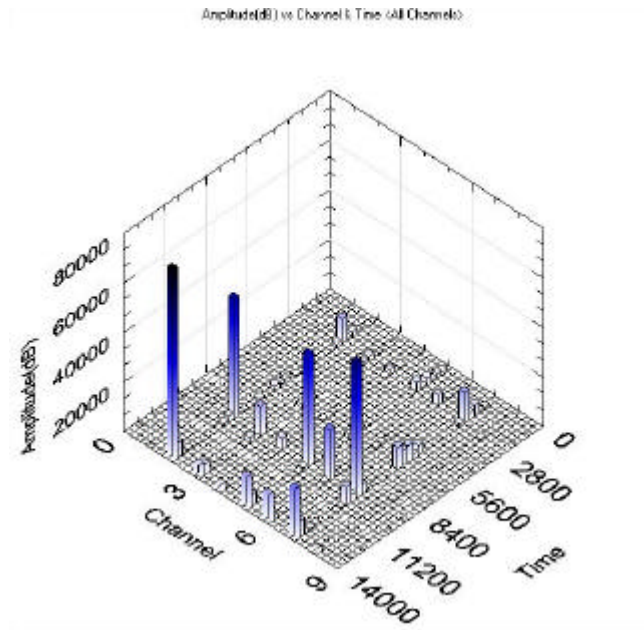


**Figure 28**  
Amplitude, channel, time - loading of February 13, 2003 (loading No. 1, entire test)

## Finite Element Modeling

Finite element models of the test specimen were developed using the representative volume element (RVE) approach as described previously in this report. To determine the validity of these finite element models pin and roller type supports were first modeled at the longitudinal centerline of the bearing pad supports. Loads of 6,000 and 82,000 pounds were applied as pressure loads over an area of 22 inches x 12 inches to simulate the bearing pad condition at the loading points.

The equations and calculations used to determine the analytically predicted deflection of the beam specimen are shown below.

$$D = b \left[ \frac{(d-t)^2 t}{2} E_f + \frac{(d-2t)^3}{12} E_c \right] \quad (1)$$

where:

D = bending stiffness of test specimen

b = width of beam = 12"

d = total depth of beam = 35.0"

t = face thickness = 0.50"

$E_f$  = modulus of face sheet in longitudinal direction = 3,191,000 psi

$E_c$  = modulus of equivalent core = 49,458 psi

Therefore,

$$D = 12.0 \left[ \frac{(35.0 - 0.50)^2 * 0.50}{2} (3,191,000) + \frac{[35.0 - 2(0.50)]^3}{12} (49,458) \right] = 13,338,160,482 \text{ lb} \cdot \text{in}^2$$

Face shear deformations were approximated by assuming that the facesheet shear stiffness was equal to that of the honeycomb core. This approximation has a minor affect on the results.

Midspan deflection due to bending and shear is then:

$$\delta = \frac{Pa}{24D}(3L^2 - 4a^2) + \frac{f_s Pa}{GA} \quad (2)$$

where:

P = applied load at each loading point (6,000 lbs.)

a = dimension from end of bearing to applied load = 85.5"

L = span length = 362"

$f_s$  = shape factor (1.2 for rectangular shape)

G = shear modulus of equivalent core = 34,374 psi

A = area of equivalent core + facesheets = 35" \* 12" = 420 in<sup>2</sup>

For the case investigated the resulting analytical deflection at midspan is:

$$\delta = \frac{6,000(85.0)}{24(13,338,160,482)} \{3(364)^2 - 4(85.0)^2\} + \frac{1.20(6,000)(85.0)}{34,374(420)}$$

$$\delta = 0.59" \text{ (flexure)} + 0.04" \text{ (shear)} = 0.63"$$

The midspan deflection as predicted by the RVE finite element model was also 0.63 inches as shown in figure 29 (finite element displacement results are shown in millimeters).

An identical model was run for the case with 82,000 pounds at each loading point (figure 30). Since only linear behavior was considered in the finite element models similar comparisons between analytical and finite element model results were achieved.

The bearing pads used on the Tulane beam specimen had dimensions of 0.79" by 12.5" by 22" as described previously. These large bearing pads had a significant impact on the behavior of the test specimen. The modeling of bearing pads in the finite element models is described in more detail in references [7] and [8]. Finite element models were developed that incorporated these bearing pads at the supports for both the 6,000 and 82,000 pound load

cases as shown in figures 31 and 32. The deflection as predicted by the finite element model at 6,000 pounds resulted in good agreement with the measured deflections at this level of load when the effect of the compression of the bearing pad support was considered. At the failure load of 82,000 pounds, the finite element model was significantly stiffer than the behavior of the test specimen. This was to be expected because the non-linear behavior of the specimen as indicated in figures 17 and 18 was not incorporated into the finite element models. This non-linear behavior is due primarily to the accumulation of damage in the specimen at higher levels of ultimate load. A more thorough analysis of the data indicates that this damage begins to occur at approximately 25,000 pounds. A comparison of the measured midspan deflections and those predicted by the RVE finite element models is given in table 6.

**Table 6**  
**Midspan deflection (inches)**

<b>Load at each point</b>	<b>6,000 pounds</b>	<b>82,000 pounds</b>
RVE model	0.41	5.59
Experimental	0.38	6.10
Percent Difference	+ 7.8	-9.1

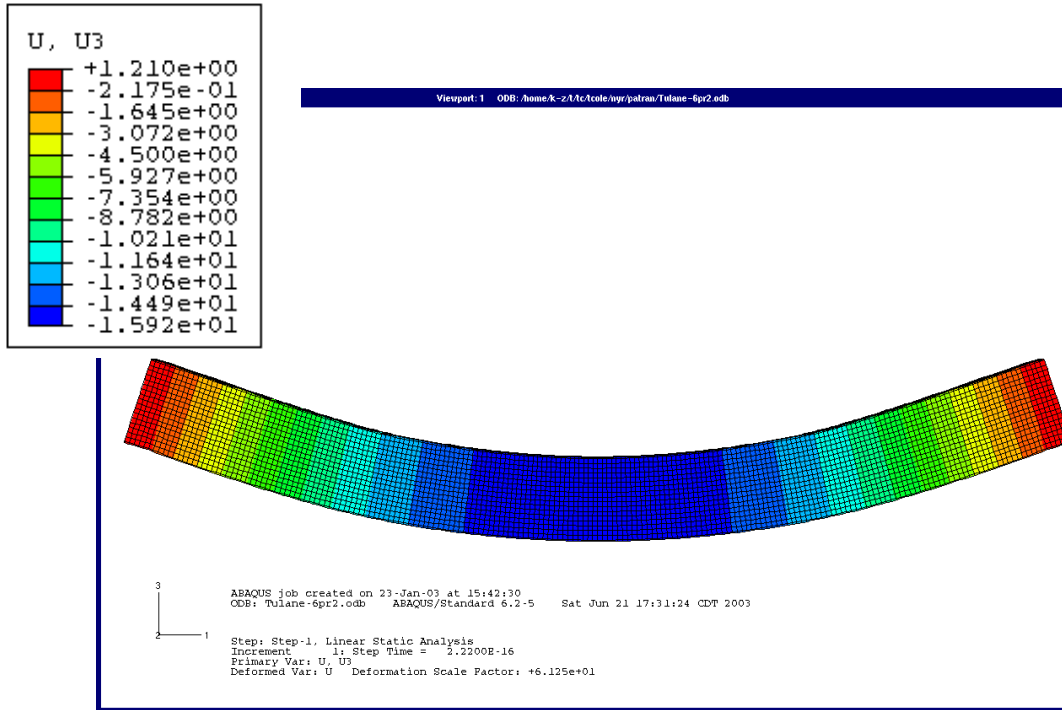


**Figure 29**  
**Vertical displacement at 6,000 pounds - pin and roller supports**

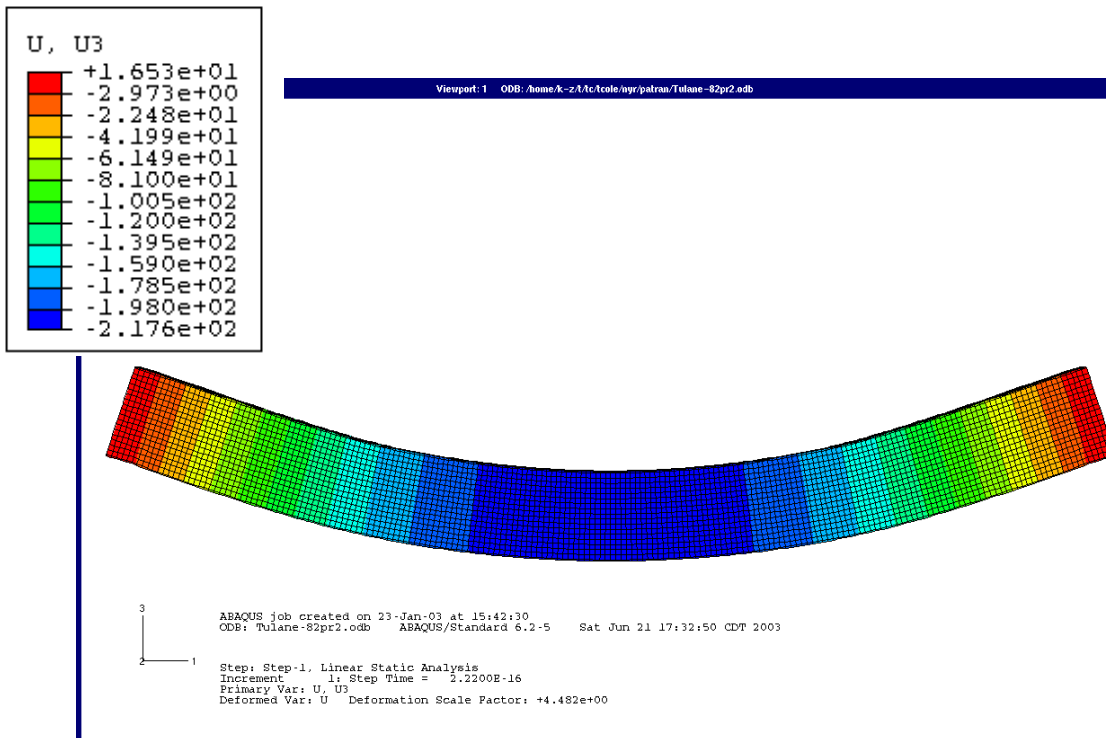


**Figure 30**  
**Vertical displacement at 82,000 pounds - pin and roller supports**

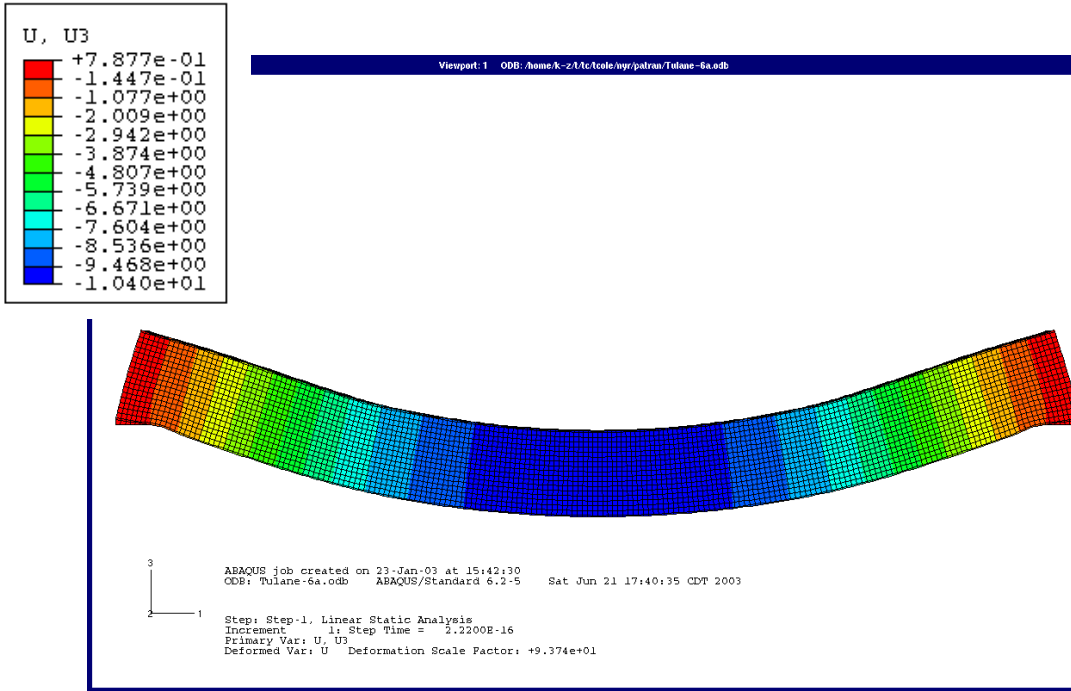


**Figure 31**  
**Vertical displacement at 6,000 pounds - bearing pad supports**

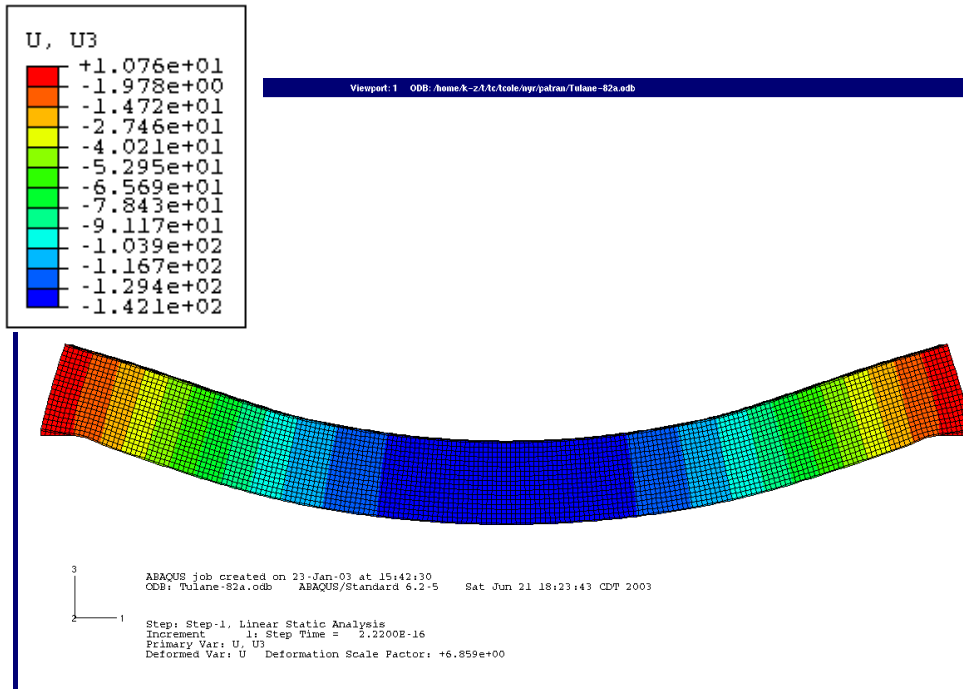


**Figure 32**  
**Vertical displacement at 82,000 pounds - bearing pad supports**



## CONCLUSIONS

The following conclusions can be drawn based on the results described:

1. Acoustic emission monitoring indicated that little or no significant damage occurred in the specimen as a result of the fatigue loading to 2 million cycles.
2. The first sign of significant damage to the specimen as defined by the presence of the Felicity effect occurred at approximately 35,000 pounds. This was approximately 40 percent of the ultimate load.
3. Acoustic emission monitoring provided insight into the progression of damage in the specimen. Damage appeared to begin inside the loading points and then to progress to the ends of the specimen.
4. The results of the finite element model agreed well with experimentally measured results. The simplifications used in the representative volume element approach had a minimal effect on the results obtained.



## RECOMMENDATIONS

The following recommendations are made based on the results of the research program:

1. While the acoustic emission monitoring described provided insight into the damage locations and damage progression in the specimen, the results were limited by the number of sensors used. It is recommended that sensor spacing on future projects be based on recommendations given in reference [1] if practicable.
2. Since acoustic emission monitoring can provide insight into damage progression in fiber reinforced polymeric components, it is recommended that acoustic emission monitoring be implemented on future research projects involving FRPs.
3. The representative volume element approach for similar honeycomb specimens can be used with confidence for two-dimensional loading cases. Additional research is necessary to validate the approach for three-dimensional loading cases.

While the data gathered and the interpretation of the data was useful for this project, it is noted that acoustic emission monitoring in particular and structural health monitoring in general are progressing fields. Future research in acoustic emission monitoring should focus on pattern recognition techniques and other methods to advance data interpretation. Correlations should be pursued between acoustic emission data and useful service life of civil engineering structures. Future applications for acoustic emission monitoring should not be limited to fiber reinforced polymers and should include prestressed and reinforced concrete structures.



## ACRONYMS, ABBREVIATIONS, & SYMBOLS

a = dimension from end of bearing to applied load

A = area of equivalent core + facesheets

AE = acoustic emission

b = width of beam

d = total depth of beam

dB = Decibel

D = bending stiffness

$E_f$  = modulus of face sheet in longitudinal direction

$E_c$  = modulus of equivalent core

$f_s$  = shape factor

FRP = fiber reinforced polymer

G = shear modulus of equivalent core

Hz = hertz

L = span length

micro-strain = engineering strain  $\times 10^6$

msi = million pounds per square inch

P = applied load at each loading point (6,000 lbs.)

PAC = Physical Acoustics Corporation

R15I = Resonant acoustic emission sensor (150 kHz resonant frequency, integral 40 dB preamplifier)

RVE = Representative Volume Element

t = face thickness



## REFERENCES

1. The Committee on Acoustic Emission from Reinforced Plastics (CARP), "Recommended Practice for Acoustic Emission Evaluation of Fiber Reinforced Plastic (FRP) Tanks and Pressure Vessels," *a Division of the Technical Council of The American Society for Nondestructive Testing, Inc.*, 1999.
2. American Society of Mechanical Engineers, "Reinforced Thermoset Plastic Corrosion Resistant Equipment," *ASME RTP-1*, 1999 Edition.
3. ASME Subcommittee on Fiber-Reinforced Plastic Pressure Vessels, "Section X: Fiber-Reinforced Plastic Pressure Vessels," *ASME Boiler and Pressure Vessel Code*, 1998 Edition.
4. Ohtsu, M., Uchida, M., Okamoto, T., and Yuyama, S., "Damage Assessment of Reinforced Concrete Beams Qualified by Acoustic Emission," *ACI Structural Journal*, July-August 2002, pp. 411-417.
5. Yuyama, S., Okamoto, T., Shigeishi, T., Ohtsu, M., and Kishi, T., "A Proposed Standard for Evaluating Structural Integrity of Reinforced Concrete Beams by AE," *Acoustic Emission: Standards and Technology Update, ASTM, STP 1353*, 1998, pp. 25-40.
6. Johnson, D., Shen, H., and Finlayson, R., "Acoustic Emission Evaluation of Reinforced Concrete Bridge Beam with Graphite Composite Laminate", 2001 (*internal copy*).
7. Cole, T., "Finite Element Modeling and Experimental Testing of an FRP Bridge Specimen," Masters Thesis for the Department of Civil Engineering, Tulane University, August, 2003 (*expected*).
8. Ziehl, P., and Cole, T., "Finite Element Modeling of FRP Bridge, Troupsburg, New York," Final Report and Addendum submitted to the New York Department of Transportation, June and August, 2002.
9. Kalny, O., Ziehl, P., Peterman, R. and Cole, T., "Computational Models for Deflection Response of FRP Sandwich Panels with Honeycomb Core," *ASCE Journal of Composites for Construction (in preparation)*.
10. Ziehl, P. and Cole, T., "Finite Element Analysis and Nondestructive Evaluation of FRP Honeycomb Bridge System," *ASCE Journal of Bridge Engineering (in preparation)*.
11. Plunkett, J. D., "Fiber Reinforced Polymer Honeycomb Short Span Bridge for

- Rapid Installation,” *NCHRP-IDEA Project Report*, 1997.
12. Lopez, M., “Experimental Testing of FRP Beam Specimen,” Final Report submitted to the New York Department of Transportation, 2002.
  13. Davalos, J.F., et al., “Modeling and Characterization of Fiber-Reinforced Plastic Honeycomb Sandwich Panels for Highway Bridge Applications,” *Composite Structures*, Volume 52, Number 3-4, May/June, 2001, p. 441-452.
  14. Abaqus, Version 6.2, Pawtucket, RI: Hibbitt, Karlsson & Sorenson, Inc., 2001.
  15. Patran, Version 2000 r.2, Santa Ana, CA: MSC Software Corp., 2000.
  16. Ulloa, F. and Ziehl, P., “Acoustic Emission Monitoring of Fiber Reinforced Beams with Concrete Slabs,” *Proceedings of the ASNT 9<sup>th</sup> Annual Research Symposium*, Birmingham, AL, 2000.
  17. Ziehl, P., “Acoustic Emission Evaluation of FRP Bridge Beams,” submitted to the Texas Department of Transportation, February and July 2003.
  18. ASTM E 1316-00, *Standard Terminology for Nondestructive Examinations*, American Society of Testing and Materials, Pennsylvania, USA, 2000.
  19. Fowler, T., and Gray, E., “Development of an Acoustic Emission Test for FRP Equipment,” *American Society of Civil Engineers Convention and Exposition*, Boston, April 1979.
  20. Ziehl, P., “Development of a Damage Based Design Criterion for Fiber Reinforced Polymer Vessels,” Dissertation for the Department of Civil Engineering, The University of Texas at Austin, December, 2000.